NASA TECHNICAL REPORT

NASA TR R-272

C.1

NASA TR R-272

RADIOMETRIC BORESIGHTING BY SEQUENTIAL LOBING

by George G. Haroules and Wilfred E. Brown III

Electronics Research Center
Cambridge, Mass.

NATIONAL AERONAUTICS AND SPACE ADMINISTRATION • WASHINGTON, D. C. • OCTOBER 1967

RADIOMETRIC BORESIGHTING BY SEQUENTIAL LOBING

By George G. Haroules and Wilfred E. Brown III

Electronics Research Center
Cambridge, Mass.

NATIONAL AERONAUTICS AND SPACE ADMINISTRATION

For sale by the Clearinghouse for Federal Scientific and Technical Information
Springfield, Virginia 22151 – CFSTI price $3.00

RADIOMETRIC BORESIGHTING BY SEQUENTIAL LOBING

By George G. Haroules and Wilfred E. Brown III
Electronics Research Center

SUMMARY

Analytic expressions for the angular error signals from sequentially lobed antenna beams in a radiometric mode of operation are derived and verified experimentally.

The suppression of antenna sidelobe contributions and discrimination against the atmospheric reradiation component are discussed.

The results of an experimental observation program are presented in support of the analysis of the sequential lobing technique.

INTRODUCTION

Future deep-space communication systems have directed increased attention to methods for measuring the performance characteristics of large-aperture antenna systems. The Fresnel zone extent of large antenna systems precludes the use of instrumented aircraft or tethered balloons to measure antenna patterns, radio boresight, structural performance, and aperture efficiency of such large antennas. However, a radiometric boresight tracking signal of high precision would permit evaluation of such characteristics through direct comparison of the indicated radio position of the antenna beam as a function of time with the known position of the radio star.

Radio sources can be used as targets of opportunity to generate a high precision radiometric boresight tracking signal because of their relatively high flux intensity, small angular size and fixed celestial coordinates.

The investigation described in this report was conducted to evaluate a sequentially lobed radiometric technique for application in future deep-space communication systems. The objective of the program was to obtain a precise, angle-tracking error signal as opposed to a relatively simple first-order cancellation of the atmospheric component. A significant improvement in reducing antenna sidelobe effects also occurred. The suppression of antenna sidelobe contributions and discrimination against the atmospheric reradiation component suggests the utility of the technique for the measurement of refractive angle bending.

BORESIGHT AND ANGULAR SENSITIVITY

Directive antennas often require precise determination of the direction of the beam on the tracking axis, based on an electrical indication from the antenna system (ref. 1); such a direction is called the "electrical boresight." This direction is determined with respect to some reference direction, called the "reference boresight," which may be a specified stationary direction, or may be obtained from the antenna by a physical indication such as an optical or mechanical axis, or by a prior electrical indication. Measurements of boresight error are concerned with the angular deviation of the electrical boresight of an antenna from its reference boresight. Based on such measurements, it may be necessary to adjust the antenna system to minimize boresight error, or to place the electrical boresight in alignment or perpendicularity with mechanical axes or another physical reference.

SEQUENTIAL LOBING

The beam direction (ref. 1) of an antenna with a single, major lobe is usually determined by noting the direction of maximum response, or the direction halfway between equal responses either side of the peak. The precision of such determination is usually in the order of one-tenth the half-power beamwidth.

Much greater precision of direction is obtained where two or more overlapping beams or lobes are provided as indicated in Figure 1. These lobes are compared to indicate a common direction by equality of amplitude or phase. When the comparison is done sequentially, it is termed sequential lobing (ref. 2) and typically compares amplitude; two examples of this class are conical scanning and lobe switching. When the comparison is done simultaneously, it is called simultaneous lobing or monopulse (Figure 2); in this case, either amplitude or phase may be compared (ref. 3). The precision of determination of electrical boresight with such antennas can be better than about 0.01 the beamwidth of an individual lobe.

RADIOMETRIC SEQUENTIAL LOBING

A radiometric sequential lobing technique can be described as two paired sets of antenna beams in orthogonal coordinates about the boresight axis as shown in Figure 3. Each paired set of beams is processed by a separate radiometric receiver and is used to derive the algebraic sum of the power obtained from the dual antenna beams in that coordinate. A functional block diagram of a single-channel, sequentially lobed radiometric tracker is shown in Figure 4. The operation of each radiometric channel is such that the power received by one beam provides a positive voltage at the receiver output while the other

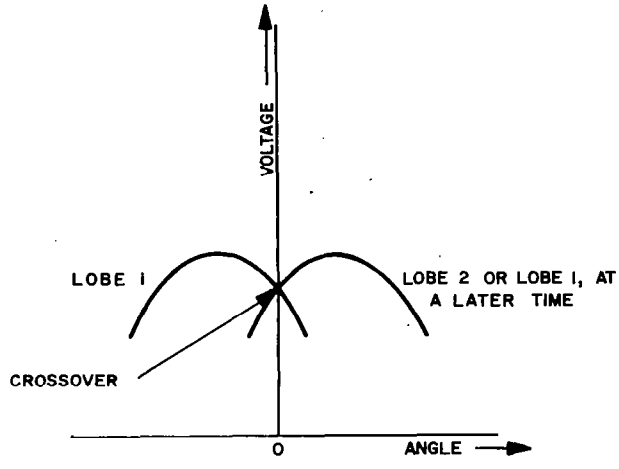

Figure 1. – Lobe patterns, sequential, monopulse, or conical scanning

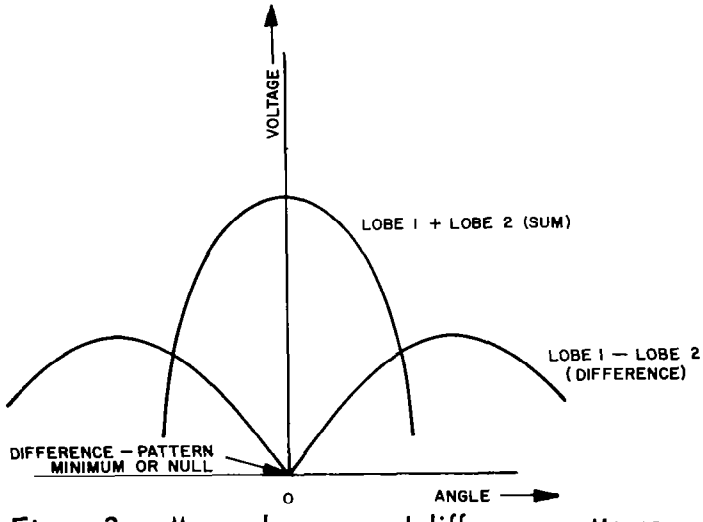

Figure 2. – Monopulse sum and difference patterns

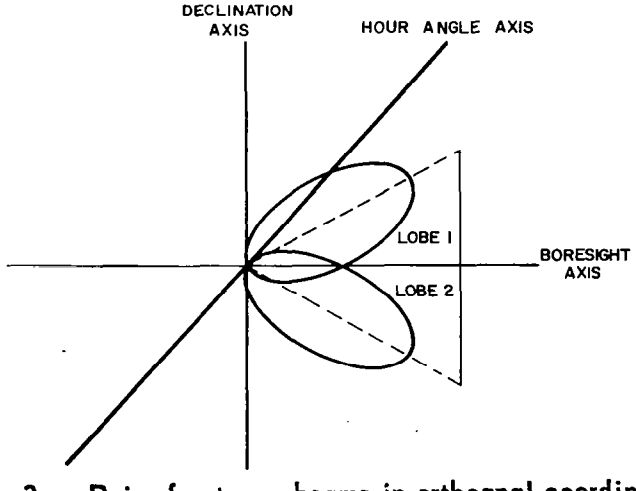

Figure 3. – Pair of antenna beams in orthognal coordinates

beam provides a negative voltage output. The "3-db circles" of the antenna pattern created by two paired sets of antenna beams in orthogonal coordinates is shown projected on the celestial sphere in (Figure 5) for an equatorially mounted antenna system. When the target passes along the line of centers of either beam, a precision tracking signal is generated. The analytical derivation of this tracking signal, known as an "S" curve, is discussed in Appendix A.

HIGH-PRECISION TRACKING SIGNAL

When sequential lobing is applied to the radiometric boresighting of large aperture antenna systems, the resulting "S" curve may be used as a high-precision tracking signal. The derivation of a tracking signal of this type is typical of the family of monopulse techniques and permits the structural performance of a large antenna system to be evaluated by directly comparing the indicated radio position of the antenna beam as a function of time with the known position of the radio source. The greatest accuracy is achieved when the slope of the "S" curve is a maximum for a source on radio boresight. This occurs when ϕ_B equals $2\phi_A$ or

$$T'_A \Big|_{\phi_s = 0} = -\frac{2\pi}{\phi_B} \sin\left(\frac{\pi \phi_A}{\phi_B}\right) T_{s(\theta,\phi)} e^{-\tau \sec \theta_s} \qquad (1)$$

where

ϕ_A = the separation between the peaks of the antenna beams

ϕ_B = the angular size of either of the antenna beams

ϕ_s = the angular position at the source

θ_s = the elevation angle measured from the zenith

τ = the vertical opacity of the atmosphere

T'_A = the rate of charge of equivalent antenna temperature

T_s = the source temperature, ^oK.

Thus, when the radio beams are crossed at the 3-db points, the slope is given by:

$$T'_{ant.} \Big|_{\phi_s = 0} = \left(\frac{\pi}{\phi_A}\right) T_s \, e^{-\tau \sec \theta_s} = \frac{\pi \, T_A}{\phi_A} \quad . \qquad (2)$$

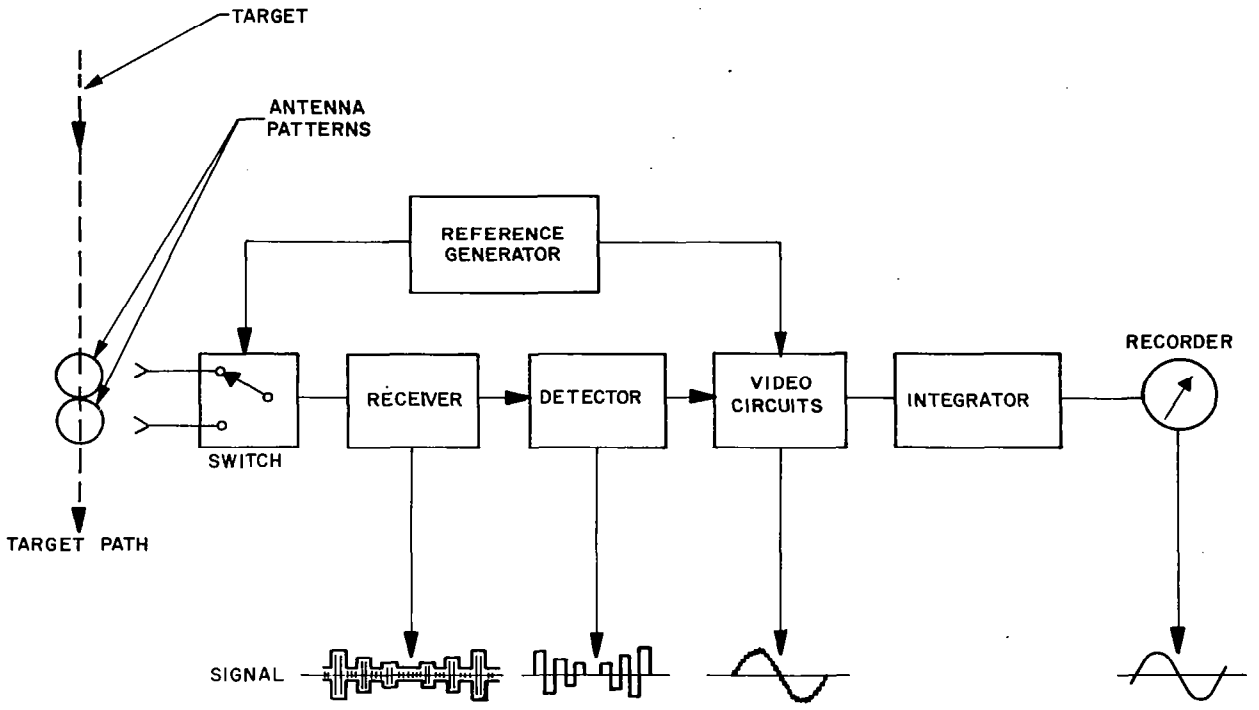

Figure 4. – Sequentially lobed radiometric tracker (one dimension)

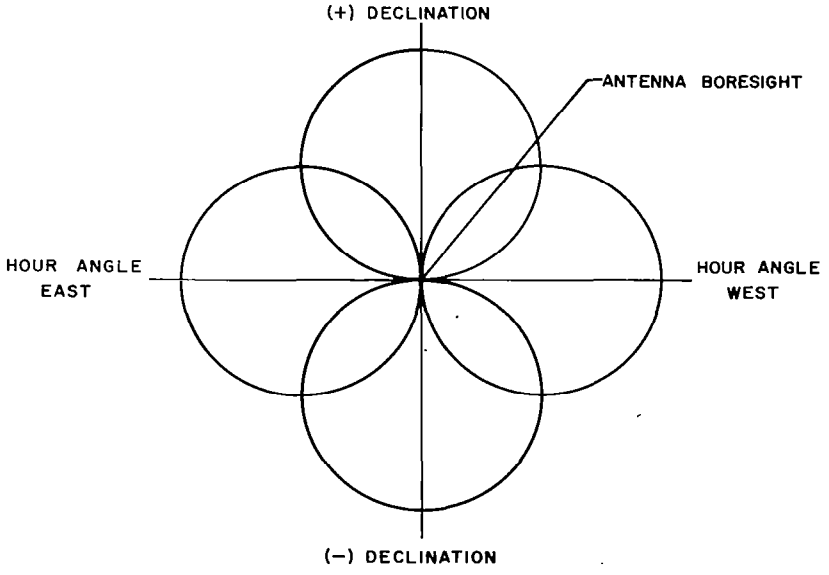

Figure 5. – Projection of "3-db circles" of antenna pattern on the celestial sphere

The expected angular rms tracking accuracy may be expressed in terms of the sensitivity (equation (9)) of the radiometer receiving system which processes the sequentially lobed radio beams as:

$$\delta \phi_{rms} = \frac{\phi_A}{2} \quad \frac{(FL-1)T_o}{T_A} \quad \frac{1}{(t \Delta \nu)^{1/2}} \tag{3}$$

where

T_A = the equivalent antenna temperature

F = the receiver noise figure

L = the RF losses

T_o = 290^o K

t = the post-detection integration time constant RC

$\Delta \nu$ = the instantaneous bandwidth.

From this equation it is clear that the peak-to-peak amplitude of the "S" curve and the peak-to-peak amplitude of the noise of fluctuations superimposed on that curve provide a direct measure of angle-tracking capability. The rms tracking capability is related to these two parameters of the "S" curve and the angular separation of the two antenna beams by the expression:

$$\delta \phi_A = \frac{\phi_A}{3 \pi M_s} \tag{4}$$

where M_s, the figure of merit of the "S" curve, is given by the expression:

$$M_s = \frac{\text{"S" curve peak-to-peak amplitude}}{\text{peak-to-peak noise fluctuations}} \tag{5}$$

where the peak-to-peak noise fluctuations are six times the sensitivity of the radiometer.

LIMITATIONS CAUSED BY ATMOSPHERIC EFFECTS

Those characteristics of the Earth's atmosphere which most seriously affect the performance of a sequentially lobed antenna system are attenuation, reradiation, and refraction. Attenuation and reradiation affect the slope of the tracking error signal and the position of null output in elevation.

Refractive effects do not directly perturb the tracking error signal. As a result, sequential lobing can be used to measure refractive angle bending by comparing the indicated celestial coordinate position of a radio source with its known position as a function of the elevation angle of observation.

The paired radio beams of a sequentially lobed radiometric antenna boresighting system sense a sky temperature difference as a consequence of the elevation angle dependence of the intensity of the atmospheric reradiation component. An approximate expression for this temperature difference obtained by assuming identically narrow antenna beams is:

$$\Delta T_{unbalance} = T_{atm}\left[e^{-\tau \sec\left(\theta_s + \frac{\theta_A}{2}\right)} - e^{-\tau \sec\left(\theta_s - \frac{\theta_A}{2}\right)}\right] \quad (6)$$

where

T_{atm} = the effective average temperature along the raypath through the atmosphere.

θ_A = angular size of the antenna beams

θ_S = the zenith angle or the elevation angle measured from the the zenith

τ = the vertical opacity of the atmosphere.

The error in angle boresight produced by the sky gradient is equal to the product of the atmospheric reradiation temperature difference and the reciprocal of the S-curve error function slope on the radio boresight. It may be expressed as:

$$\Delta\theta_{elevation} = \Delta T_{unbalance}\left[\frac{\pi T_A}{\theta_A}\right]^{-1}, \quad (7)$$

or the fractional antenna beam angle error is:

$$\frac{\Delta\theta_{elevation}}{\theta_A} = \frac{\Delta T_{unbalance}}{\pi T_A}. \quad (8)$$

The error associated with the sky gradient will always be toward the horizon. Additive noise balancing can be used to cancel the error associated with sky gradient by introducing an adjustable amount of noise into the transmission line which connects the feed of the upper antenna beam. An rf balance can be accomplished with the antenna pointed off the azimuth position of the radio source, but at the same elevation angle. Further discussion of this technique can be found in Appendix B.

LIMITATIONS CAUSED BY RADIOMETRIC SENSITIVITY

The sensitivity of a radiometric receiving system, i.e., the minimum detectable signal, is determined by the amplitude of the fluctuations present at the receiving system output in the absence of an input signal. These fluctuations are attributable to statistical fluctuations caused by the internal noise of the receiver, the atmosphere, celestial sources, and the spurious gain fluctuations associated with the receiver network. The amplitude of the fluctuations of the noise waveform can, in principle, be reduced to any desired degree by reducing the post-detection bandwidth (increasing the integration time constant). In practice, however, the longest usable integration time is frequently limited by the time available for observing the signal source. For example, when an antenna beam is scanned across a celestial radio source, the post-detection integration time constant and/or the antenna scanning rate are usually adjusted to provide a time between source positions at the 3-db antenna points equivalent to a minimum of six post-detection integration time constants.

The level of radiometer output fluctuations associated with receiver gain instability is directly proportional to the rf input noise unbalance sensed by the radiometer at its two input terminals. With sequential lobing, the power level sensed by the radiometer at either of the paired antenna feed outputs will, under most conditions, be very nearly the same. A reduction in system sensitivity associated with receiver gain variations operating on the temperature input unbalance of a sequentially lobed radiometer is usually negligible compared to the potential pointing error in elevation of such a system. Thus, the effect of receiver gain variations on the radiometric sensitivity of a sequentially lobed radiometer is negligible. With this mode of operation, the radiometric sensitivity is determined by the inherent system noise temperature, instantaneous predetection bandwidth, and post-detection integration time constant.

The sensitivity of the radiometric receiving system may, therefore, be expressed in the form (ref. 4):

$$\Delta T_{rms} = \frac{\beta\, T_N}{\sqrt{t(\Delta \nu)}} \tag{9}$$

where

T_N = the receiving system noise temperature

$\Delta \nu$ = the instantaneous predetection bandwidth

t = the post-detection integration time constant.

For the ideal rectangular predetection and post-detection bandpass characteristics, the proportionality factor β is $2\sqrt{2}$. For the more practical case of a rectangular predetection bandpass characteristic and tuned filter audio bandpass preceding the phase detector, the constant is $\pi/2$.

The receiving system noise temperature may be expressed in terms of the receiver noise figure F and the rf losses L, preceding the receiving system input in the form (ref. 5):

$$T_N = (FL - 1)\ T_o \tag{10}$$

where T_o is 290°K by definition. Thus, the rms radiometric sensitivity may be expressed in the more familiar form:

$$\Delta T_{rms} = \frac{\pi\ (FL-1)\ T_o}{2\sqrt{t\ \Delta\ \nu}} \quad . \tag{11}$$

LIMITATIONS CAUSED BY RADIO SOURCE FLUX INTENSITY AND ANGULAR SIZE

Radio Source Flux Intensities

The use of an effective antenna temperature to describe the noise power received by a specified antenna from a celestial radio source is common in radio astronomy. The antenna temperature of a source is determined by the source flux density at the frequency of observation and the solid angle of the source as viewed from the Earth relative to the solid angle of the antenna beam.

The analytical development of a "source antenna temperature" proceeds from the relationship between the power absorbed from a randomly polarized plane wave by a matched antenna aperture in the direction of the incoming wave and the flux density of the wave. If the flux density of the randomly polarized wave is S, and the effective antenna aperture is A, then the power per unit bandwidth absorbed by the aperture is given by the expression

$$P \equiv 1/2\ SA\ . \tag{12}$$

Recalling that, at microwave and millimeter frequencies, the brightness of a radio source is describable by the Rayleigh Jean's approximation of the Planck Law of radiation for a blackbody, we may, through antenna equilibrium considerations, equate the power received per unit bandwidth by the antenna to an equivalent Johnson noise power per unit bandwidth kT_A where T_A is now the "effective" antenna temperature of the source. Most radio sources do not demonstrate blackbody radiation characteristics, i.e., the source of radiation is definitely non-thermal in origin. The flux density of a radio source is, however, conventionally described in terms of the temperature of "an effective blackbody" which provides an equivalent flux density at the frequency of observation.

Consequently, the Johnson noise power per unit bandwidth obtained from a purely resistive load immersed in a thermal bath, at a temperature equivalent to the effective antenna temperature of a radio source, is identical to that received by the antenna aperture when viewing the source. This relationship may be expressed in the form:

$$kT_A = 1/2\ SA \tag{13}$$

where k is Boltzmann's constant.

For a radio source of known flux density S, the effective antenna temperature obtained by an antenna of aperture area A is then:

$$T_A = \frac{SA}{2k} \tag{14}$$

Radio Source Angular Size

The angular size of the radio source is one of the least accurately known parameters, since it is intimately related to the observer's knowledge of his own antenna pattern characteristics. The determination of radio source size has, in general, been accomplished by a "boot-strapping" process, in which an estimated angular size for several radio sources is used to determine antenna beam characteristics, and the estimate of antenna beam characteristics is, in turn, used to determine the angular sizes of other radio sources. In recent years, the observation of planets by large pencil beam antennas has improved knowledge of radio source angular size considerably (ref. 6). It is now generally agreed that the angular diameter of the radio source Cassiopeia A is of the order of 3 to 4 minutes of arc in both the North-South and East-West directions. The measured angular diameter of Taurus, however, continues to show a relatively large dispersion with reported values in the range from 3.5 to 5 minutes of arc. Cygnus A is known to be comprised of two sources spaced approximately 100 arc-seconds in the East-West direction. This source is very narrow in the North-South direction.

As we proceed to a less intense radio source, measurement data are less accurate and we encounter, as in the case of Cygnus A, sources which are quite asymmetrical insofar as their angular projection on the celestial sphere. This is of little concern in the boresighting of equatorial or polar-mounted radio telescopes. However, an elevation-over-azimuth-mounted antenna system will experience an angular rotation of a celestial source about the boresight axis as the source moves in its apparent diurnal motion from East to West. It is clear that the symmetry of the antenna pattern becomes a critical factor in this case.

EXPERIMENTAL MEASUREMENTS

The specific objectives of the experimental program were, first, to obtain a measure of the signal-to-noise characteristics of observed sources,

while determining the "S" curve tracking error and, second, to determine the effectiveness of sequential lobing in cancelling the reradiation component of the atmosphere, while suppressing the sidelobe effects of the antenna.

The instrumentation consisted of a single-channel tuned radio frequency (TRF) radiometer installed at the focal plane of an equatorially mounted, 28-foot-diameter parabola. A simplified functional block diagram of the radiometric receiver is shown in Figure 6. The predetection receiving bandwidth was 1 gHz centered at 8 gHz. The input switch or modulator was a switchable Faraday four-port rotator. The calibration signal was provided by an argon discharge noise source fed via the side arm of a 30-db coupler to provide a noise injection level of 10°K at radiometer input port A. The overall gain of the tunnel diode amplifier was 54 db, provided by four cascaded tunnel diode amplifier stages. The 1 kHz modulation frequency component at the output of the tunnel diode detector was amplified and the fundamental component synchronously detected. Following d.c. amplification and integration, the radiometer output was fed to a strip-chart recorder. System sensitivity, based on laboratory tests prior to installation and confirmed in the operational configuration when installed on the telescope, was 0.04°K rms for a post-detection integration time constant of 1 second.

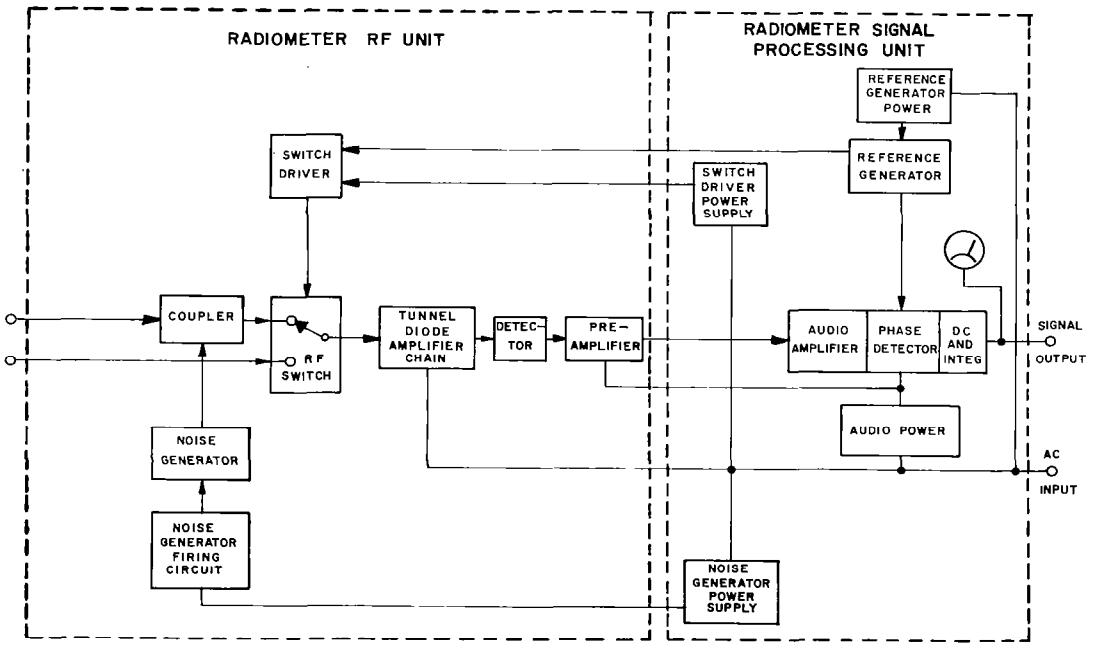

Figure 6. – Functional block diagram of radiometric receiver

Observations were conducted by scanning the antenna beams through the position coordinates of the celestial sources: Cassiopeia A, Taurus A, Cygnus A, Omega (M17), and the planet Venus. A composite of typical analog records obtained for the various radio sources and the planet Venus is shown in Figure 7. The peak-to-peak amplitudes of celestial source S-curves were each referenced to the amplitude obtained for Taurus A. Corrections were applied for atmospheric extinction by reducing all source/calibration signal ratios to the

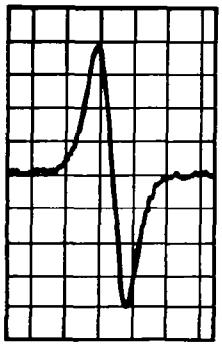

CASSIOPEIA A
(SCALE x 1)

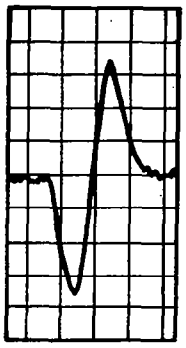

TAURUS A
(SCALE x 1)

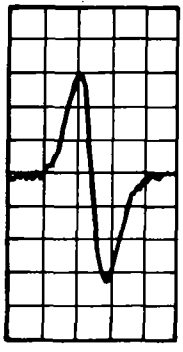

M17 (OMEGA)
(SCALE x 1)

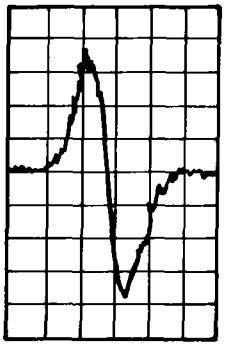

CYGNUS A
(SCALE x 2.5)

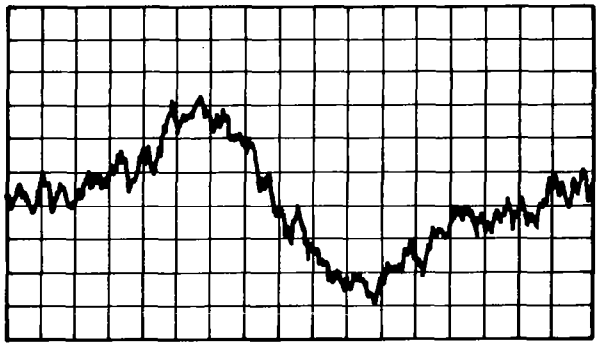

VENUS
(18 FEBRUARY 1966, SCALE x 10)

Figure 7. – "Typical" S–Curves of celestial radio sources (28–foot diameter antenna, 8 gHz)

zenith position. Correction factors for antenna beam smoothing and polarization to accommodate the angular size of the various sources relative to the antenna beam angle and the non-random polarization of Taurus and Cygnus were introduced in accord with the procedure of Baars et al (ref. 7). These correction factors are summarized in Table I. The ratios of the measured radio source flux densities relative to Taurus A are summarized in Table II. Current published values are shown in Table III.

The conjunction of Venus, which occurred before the observational program was begun, presented an excellent opportunity to evaluate the technique of sequential lobing in discriminating against the sky temperature variations. The brightness temperature of the planet for each day of observation was obtained from the expression:

$$T_B(\nu) = \frac{\lambda^2 S(\nu, t)}{2k\,\Omega_{\varphi}(t)}$$

where

$S(\nu, t)$ = the flux density (watt/m^2/Hz)

k = Boltzmann's constant, 1.38×10^{-23} (watt/Hz/^oK)

λ = wavelength of observation

$\Omega_{\varphi}(t)$ = solid angle subtended by planet.

The flux density $[S(\nu, t)]$ of the radiation received from the planet was obtained by comparing the received signal intensity with that of Taurus A on each day of observation. The flux density of Taurus A was assumed to be 581×10^{-26} watt/m^2/Hz (ref. 7). To minimize errors associated with the time variability of atmospheric extinction between the time of planet transit and transit of the radio

TABLE I

RADIO SOURCE CORRECTION FACTORS*

Source	Size	Polarization
3C461 (Cass A)	1.018	1.000
3C405 (Cygnus A)	1.000	0.974
3C144 (Taurus A)	1.036	0.980
M-17 (Omega)	1.074	1.000

*Ref. 7

TABLE II

OBSERVED RADIO SOURCE FLUX DENSITY RATIOS

Source	Observed Source to Calibration Ratio	S_s/S_{Taurus} (Haroules, Brown) 1966.2
3C461 (Cass A)	1.022	1.108 $\pm$ 2%
3C405 (Cygnus A)	0.378	0.392 $\pm$ 2%
3C144 (Taurus A)	0.906	1.000
M-17	0.815	0.931 $\pm$ 3%

TABLE III

PUBLISHED RADIO SOURCE FLUX DENSITY RATIOS

Source	S_s/S_{Taurus} (ref. 7) Heeschen 1961.1 (Corrected to 1966.2)	S_s/S_{Taurus} (ref. 7) Haddock 1964.4 (Corrected to 1966.2)
3C461 (Cass A)	1.21 $\pm$ .9%	1.08 $\pm$ 5%
3C405 (Cygnus A)	0.405 $\pm$ 10%	0.374 $\pm$ 5%
3C144 (Taurus A)	1.000	1.000
M-17	-	-

source Taurus A, the ratio of the planet signal intensity relative to Cygnus A and Cassiopeia A was measured on each day of observation and introduced in the data reduction process. The brightness temperature of the planet Venus derived from these measurements was 560°K + 20°K and is plotted as a function of the data observation in Figure 8. Phase-angle-dependent variations in the observed brightness temperature as a function of amplitude were below the limit of error in our measurements and could not be detected.

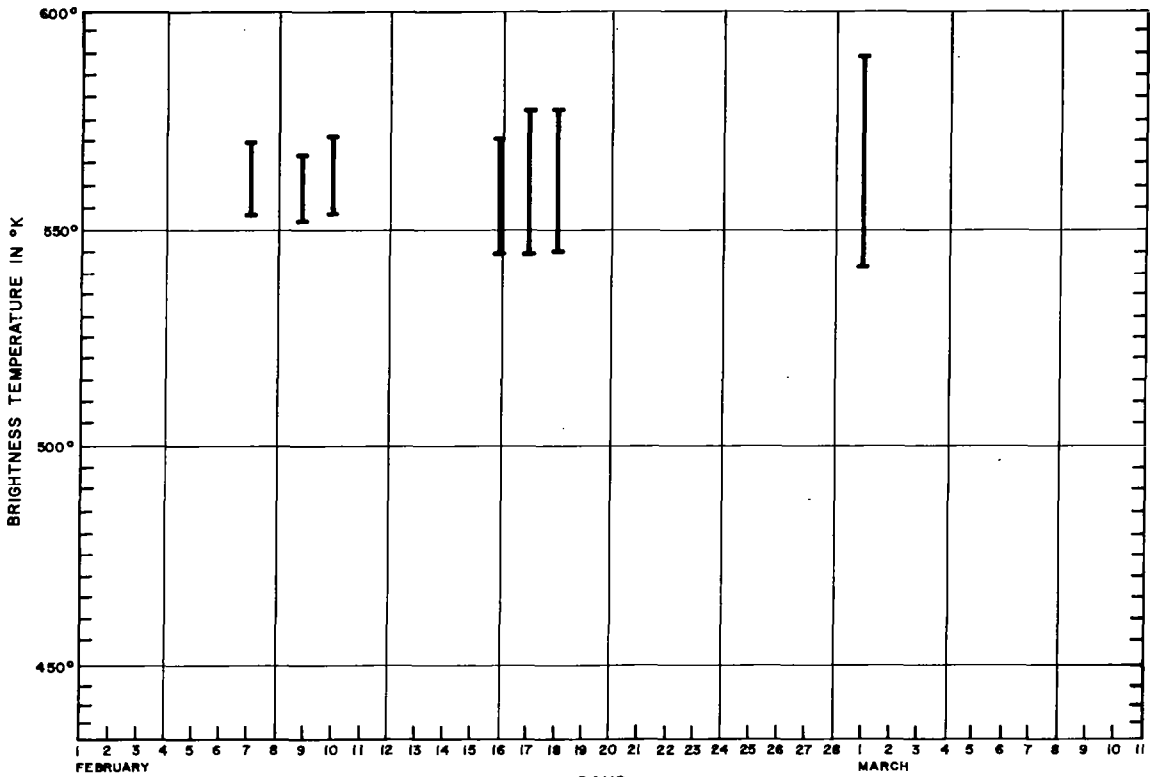

Figure 8. – Venus brightness temperature

CONCLUSIONS

Sequentially lobed antenna beams paired in orthogonal coordinates about the radio boresight axis of an antenna, when applied in a radiometric mode of operation, make it possible to track precisely the spatial centroid of broadband sources of noise typical of the signals emitted by discrete celestial radio sources. Although the antenna axis output indicator system was not sufficiently precise to provide a direct measure of angle boresighting capability, inspection of the "S" curve characteristics for Cassiopeia A shown in Figure 3 indicates a rms angle tracking capability of 2.5 arc-seconds, which is consistent with predicted performance. The effectiveness of this technique for boresighting large aperture antenna systems would be considerably enhanced by the observation of quasi-stellar objects (quasars) on account of their relatively small angular size and near coincidence with associated optical sources. Unfortunately, these ideal sources for radio boresighting were beyond the power of the instrument used in this experiment so that the more intense celestial

sources, which are not so well suited to precise antenna boresight calibration, were required.

The consistency of the data under varying weather conditions and the close agreement with published values listed in Table III attest to the effective suppression of antenna sidelobe effects. The subtraction process operating on the sidelobe power received by two slightly displaced antenna beams offers a noticeable reduction in the level of sidelobe contributions in comparison with techniques which utilized coherent multiplication to derive a simultaneous angle tracking error signal.

Excellent cancellation of the effects of the atmospheric reradiation component was noted when employing the technique of sequential lobing. Attempts to detect spatial variations in atmospheric reradiation comparable to the antenna beam size (18 arc-minutes) were unsuccessful. Several long-term patrols were made with the antenna pointing in a fixed position relative to the local framework of reference. Significant variations (greater than tangential signal) were observed only under the most adverse conditions of heavy cloud cover. Under these conditions, variations as great as $0.5^{\circ}K$ were noted at the radiometer output. Correlation of the polarity and amplitude of radiometer output variations with visually observed cloud cover characteristics in the vicinity of the radio beam was impossible. Similar experimental data obtained at higher frequencies on a coincident time base, combined with cloud density data along the ray path, should provide a quantitative measure of the applicability of this technique to the upper microwave and millimeter frequencies and, in addition, useful data concerning the frequency-dependent nature of the spatial distribution of atmospheric inhomogeneities.

Finally, sequential lobing by radiometric means simplifies the measurement of celestial source flux ratios at the higher microwave frequencies and millimeter frequencies where the effects of the reradiation component are more severe than at the longer centimeter wavelengths. Recent evidence of large fractional variations in the radio emission of quasi-stellar sources 3C273, 3C279, and 3C345 at a wavelength of 3.75 cm suggests the scientific value of higher microwave and millimeter measurements of these and similar sources over extended periods of time. Radiometric measurements of this type can be made with considerable ease using the sequentially lobed antenna beam approach, as demonstrated by the experimental measurement of several radio source flux ratios.

REFERENCES

1. Test Procedures for Antennas. IEEE No. 149, January 1965.
2. Skolnick, M.I.: Introduction to Radar Systems. McGraw-Hill, 1962, pp. 165-166; Barton, K.D.: Radar System Analysis. Prentice-Hall, October 1965, pp. 264, 311.
3. Rhodes, D.R.: Introduction to Monopulse. McGraw-Hill, 1959, pp. 7-19.

4. Kraus, J. D.: Radio Astronomy. McGraw-Hill, 1966, p. 102.

5. Tiori, M.: Radio Astronomy Receivers. PGAP, 1964; Taylor, H. P.: The Radiometer Equation. Microwave Journal, May 1967, pp. 39-42.

6. Howard, W., Moran, S.: General Catalogue of Discrete Radio Sources. Ap. J., Supplement Series No. 93, vol. 10, March 1965.

7. Baars, J.W.M., Mezger, P.G., and Wendker, H.: The Spectra of the Strongest Non-Thermal Radio Sources in the Centimeter-Wavelength Range. Ap. J., vol. 142, July 1965.

APPENDIX A

ANALYTICAL EXPRESSION FOR SEQUENTIALLY LOBED BEAMS

The power received by a single antenna beam may be expressed in terms of its equivalent antenna temperature in the form:

$$P_{abs} = kT_A \Delta \nu \tag{A-1}$$

where

P_{abs} = the power received or absorbed by the antenna

k = Boltzmann's constant (1.38×10^{-23} joule $^{o}K^{-1}$)

$\Delta \nu$ = the received bandwidth in Hz

T_A = the antenna temperature caused by the source.

The equivalent antenna temperature T_A is the integral of the actual temperature distribution weighted by the normalized antenna pattern or directivity expressed in the form:

$$T_A = \frac{1}{4\pi} \int T(\theta, \phi)\ f(\theta, \phi)\ \ d\Omega \tag{A-2}$$

where

$T(\theta, \phi)$ = the temperature distribution of source in ^{o}K

$f(\theta, \phi)$ = the normalized antenna power pattern

$d\Omega = \sin\theta\, d\phi\, d\theta$ = infinitesmal element of solid angle.

Equation (A-2) for a single beam may be expressed in the form:

$$T_A = \frac{1}{4\pi} \int_{\Omega_{mb}} T_{mb}(\theta, \phi)\, f_{mb}(\theta, \phi)\ d\Omega + \frac{1}{4\pi} \int_{\Omega_{sb}} T_{sb}(\theta, \phi)\, f_{sb}(\theta, \phi)\ d\Omega\ . \tag{A-3}$$

The two individual radio beams of a sequentially lobed radiometric system situated in slightly different orientations may be expressed in terms of individual antenna temperatures as:

$$T_{A_1} = \frac{1}{4\pi} \int_{\Omega_{mb(1)}} T_{mb(1)}(\theta,\phi)\, f_{mb(1)}(\theta,\phi)\, d\Omega + \frac{1}{4\pi} \int_{\Omega_{sb(1)}} T_{sb(1)}(\theta,\phi) f_{sb(1)}(\theta,\phi)\, d\Omega \quad \text{(A-4)}$$

$$T_{A_2} = \frac{1}{4\pi} \int_{\Omega_{mb(2)}} T_{mb(2)}(\theta,\phi)\, f_{mb(2)}(\theta,\phi)\, d\Omega + \frac{1}{4\pi} \int_{\Omega_{sb(2)}} T_{sb(2)}(\theta,\phi) f_{sb(2)}(\theta,\phi)\, d\Omega \quad \text{(A-5)}$$

where

$f_{mb(1)}(\theta,\phi)$ and $f_{mb(2)}(\theta,\phi)$ = the normalized power pattern of the main beams

$T_{mb(1)}(\theta,\phi)$ and $T_{mb(2)}(\theta,\phi)$ = the temperature distribution intercepted by the main beams

$f_{sb(1)}(\theta,\phi)$ and $f_{sb(2)}(\theta,\phi)$ = the normalized power pattern of the sidelobes and backlobes

$\Omega_{mb(1)}$ and $\Omega_{mb(2)}$ = the solid angle of the main beam

$\Omega_{sb(1)}$ and $\Omega_{sb(2)}$ = the solid angle of the sidelobes and backlobes = $4\pi - \Omega_{mb}$.

The temperature distribution of the sidelobe and backlobe structure $T_{sb}(\theta,\phi)$ is composed of atmospheric reradiation in the sidelobes $T_{atm}(1-e^{-\tau\sec\theta})$, plus the gray body radiation from the Earth. The temperature distribution of the main beam $T_{mb}(\theta,\phi)$ also contains atmospheric reradiation of the form $T_{atm}(1-e^{-\tau\sec\theta})$ in addition to the signal decreased by atmospheric extinction $(e^{-\tau\sec\theta})$.

If the two identical power patterns of a sequentially lobed system are situated in the same orientation, they will each intercept similar temperature distributions from the atmosphere and the Earth. However, in practice the sidelobes and backlobes tend to smear and lose structure as well as become small in amplitude. Thus, the power received in the sidelobes and backlobes by each power pattern of a sequentially lobed system will be equal. Sources of sufficient angular size as to be included in each main beam will also produce a null output contribution.

A switched radiometer's smoothed output indicates the average power differential presented at its two input ports. If the radiometer switching is between two power patterns of equal amplitude, a null output will result. Thus,

a discrete source passing through the individual beams of a sequentially lobed radiometric system will produce a d.c. output of appropriate polarity.

To simplify Equation (A-3), the following assumption is made based on the previous discussion that sidelobe and backlobe levels are constant and not a function of the particular coordinate system.

Therefore:

$$\frac{1}{4\pi}\int_{\Omega_{sb(1)}} T_{sb(1)}(\theta,\phi)\, f_{sb(1)}(\theta,\phi)\, d\Omega \approx \frac{1}{4\pi}\int_{\Omega_{sb(2)}} T_{sb(2)}(\theta,\phi)\, f_{sb(2)}(\theta,\phi)\, d\Omega \quad . \qquad \text{(A-6)}$$

However $T_{mb}(\theta,\phi)$ may be expressed as:

$$T_{mb}(\theta,\phi) = T_s\left(\theta_s,\phi_s\right)e^{-\tau\sec\theta_s} + T_{atm}\left(\Omega_{mb}\right)\left(1-e^{-\tau\sec\theta_s}\right) \qquad \text{(A-7)}$$

where

T_s = the equivalent antenna temperature of a discrete source

τ = the vertical atmospheric opacity

T_{atm} = the average atmospheric temperature

θ_s = the zenith angle of the source.

A first approximation is of the following form:

$$\frac{1}{4\pi}\int_{\Omega_{mb(1)}} T_{atm}\left(\Omega_{mb(1)}\right)\left(1-e^{-\tau\sec\theta_s}\right) f_{mb(1)}(\theta,\phi)\, d\Omega$$

$$\approx \frac{1}{4\pi}\int_{\Omega_{mb(2)}} T_{atm}\left(\Omega_{mb(2)}\right)\left(1-e^{-\tau\sec\theta_s}\right) f_{mb(2)}(\theta,\phi)\, d\Omega \quad . \qquad \text{(A-8)}$$

Use of Equations (A-8) and (A-6) results in the expression for the differential radiometric output ($T_{A1} - T_{A2}$) between the main beams of a sequentially lobed system.

This expression is of the form:

$$T_{A1} - T_{A2} = \frac{1}{4\pi}\int_{\Omega_{mb(1)}} T_s(\theta_s,\phi_s)e^{-\tau\sec\theta_s} f_{mb(1)}(\theta_s,\phi_s)\, d\Omega$$

$$- \frac{1}{4\pi} \int_{\Omega_{mb(2)}} T_s(\theta_s, \phi_s) e^{-\tau \sec \theta_s} f_{mb(2)}(\theta_s, \phi_s)\, d\Omega \tag{A-9}$$

$$= \frac{1}{4\pi} \int_{\Omega_{mb}} \left[T_s(\theta_s, \phi_s) e^{-\tau \sec \theta_s} \right] f_{mb(1)}(\theta_s, \phi_s) - f_{mb(2)}(\theta_s, \phi_s)\, d\Omega \tag{A-10}$$

where $\Omega_{mb(1)} = \Omega_{mb(2)}$

The effective received power pattern $f_{mb(1)}(\theta_s, \phi_s) - f_{mb(2)}(\theta_s, \phi_s)$ may be analyzed for various beam shapes. To illustrate the technique of sequential lobing analytically, a cosine squared pattern will be used to represent the shapes of the main beams. Other beam shapes requiring more complex expressions to describe their geometry may be used; however, the final result will be essentially the same.

A one-dimensional representation of the geometry of an "S" curve is shown in Figure A-1 for a cosine squared pattern where $\theta = \theta_s$. The geometry of the individual beams can be expressed in the following form:

$$\text{Beam 1} = f_{mb(1)}(\phi) = \cos^2\left(\frac{\pi}{\phi_B} \phi + \frac{\pi}{2} \frac{\phi_A}{\phi_B} \right) \tag{A-11}$$

$$\text{Beam 2} = f_{mb(2)}(\phi) = \cos^2\left(\frac{\pi}{\phi_B} \phi - \frac{\pi}{2} \frac{\phi_A}{\phi_B} \right) . \tag{A-12}$$

Therefore $f_{mb(1)}(\phi) - f_{mb(2)}(\phi)$, by the use trigonometric identities, may be expressed in the form:

$$f_{mb(1)}(\phi) - f_{mb(2)}(\phi) = - \sin\left(\frac{2\pi}{\phi_B} \phi \right) \sin\left(\frac{\pi}{\phi_B} \phi_A \right) . \tag{A-13}$$

The value of $f_{mb(1)}(\phi) - f_{mb(2)}(\phi)$ is a maximum when:

$$\sin\left(\frac{\pi}{\phi_B} \phi_A \right) = 1 \text{ or } \frac{\phi_A}{\phi_B} = 1/2 .$$

Figure A-2 describes the geometry of a 3-db crossover for a pair of sequentially lobed beams.

Equation (A-10) is now written in the following form:

$$T_{A1} - T_{A2} = \frac{1}{4\pi} \int_{\Omega_{mb}} \left[T_s(\theta_s, \phi_s) e^{-\tau \sec \theta_s} \right] \sin\left(\sin \frac{\pi}{\phi_A} \phi \right) d\Omega . \tag{A-14}$$

It should be noted that the negative sign has been dropped. In addition, it is important to note that Equation (A-14) is approximately the spatial derivative of the source distribution. This spatial derivative lends itself to the observation of lunar occultations because it deconvolves the occultation curve. Also, the ratio of the peak-to-peak value of the "S" curves obtained by observing two radio sources in a sequentially lobed mode is an accurate measure of the flux ratio of these sources when the proper extinction and source size corrections are applied.

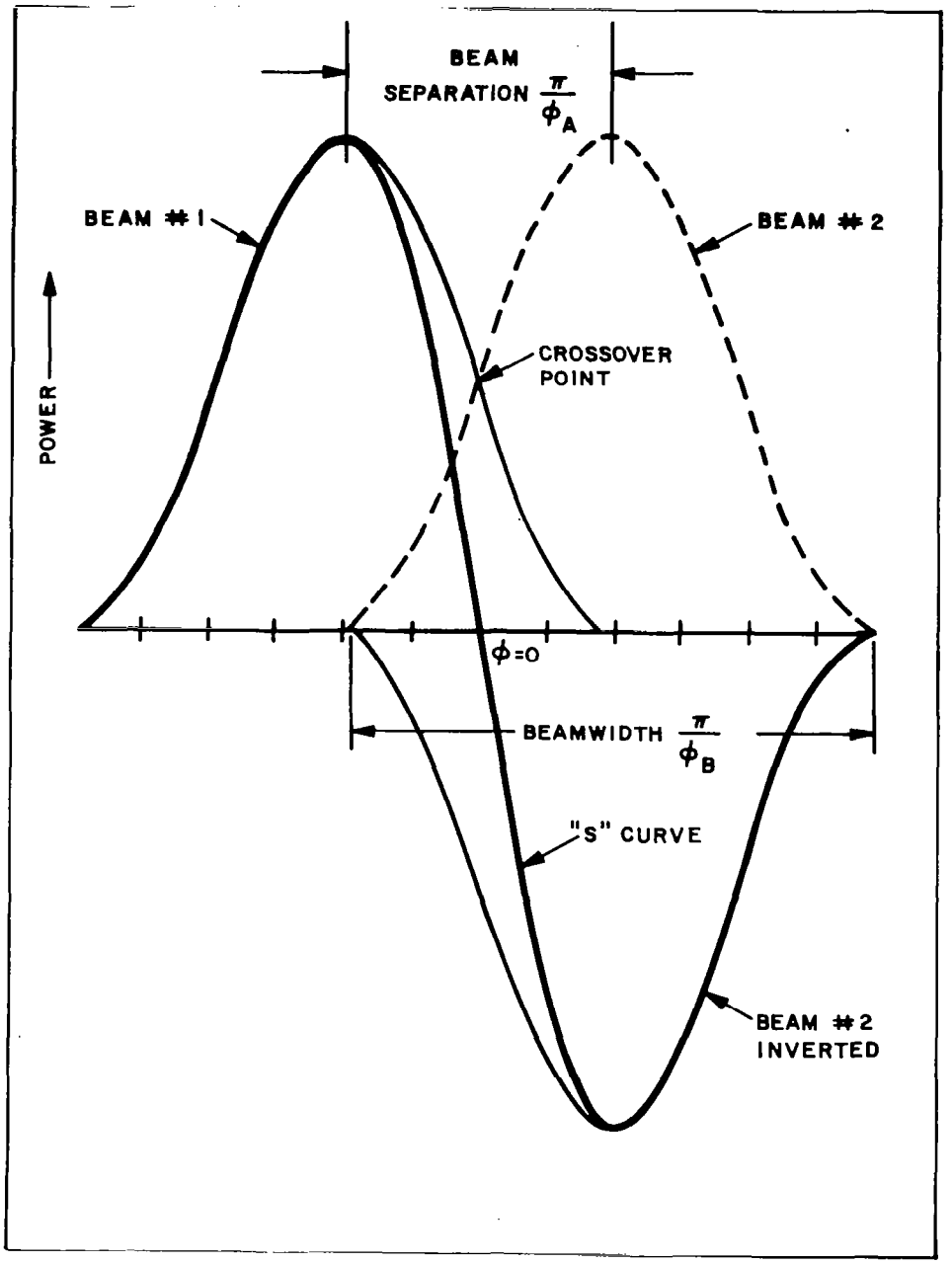

Figure A–1. – Geometrical construction of the "S–curve"

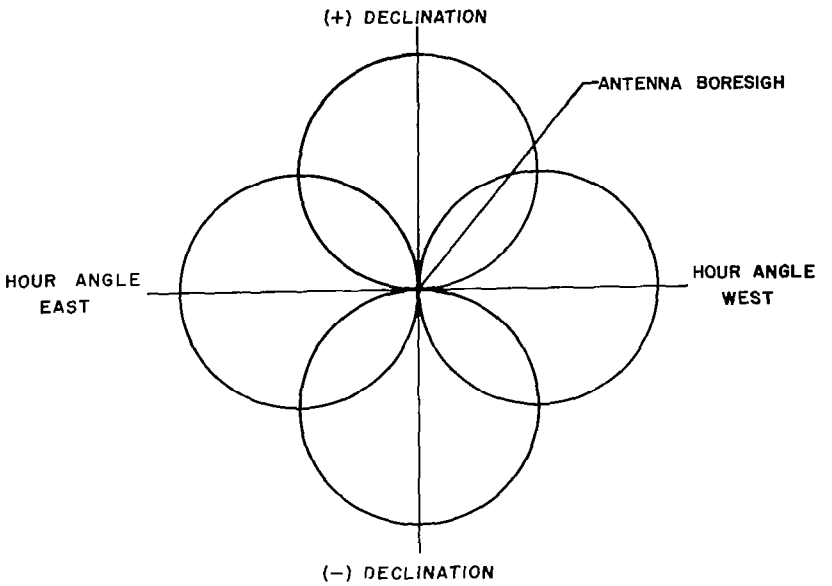

Figure A–2. – Projection of "3-db circles" of antenna pattern on the celestial sphere

APPENDIX B

ANTENNA CALIBRATION AND SKY BALANCE

A sequentially lobed radiometer must have provisions for gain calibration and zero balancing if utilized for boresight measurements. A zero mode can be provided by disconnecting the two antenna feeds and terminating the input ports of the radiometer in two loads at an equivalent temperature T_E. The switches S_1 and S_2 shown in Figure B-1 accomplish this purpose.

The receiver must be then zero-balanced to account for asymmetry in the rf transmission line and components associated with the receiver. This can be accomplished by using two calibrated terminations in a common cold bath. The known temperature between the zero reference loads and the calibration loads is used to measure the rf asymmetry.

The calibration procedure can best be represented by the following conditions.

For the zero mode the temperature appearing;

$$\text{at port A} = T_o (1 - \alpha) + T_E \alpha \quad . \tag{B-1}$$

$$\text{at port B} = T_o (1 - \beta) + T_E \beta \quad . \tag{B-2}$$

When these two temperatures are differenced by modulator switch S_3, they result in the following temperature:

$$(\beta - \alpha)\ (T_o - T_E) \ . \tag{B-3}$$

The calibration mode with the calibration source connected to S_1 and S_2 results in the following differential temperature at the output of modulator switch S_3.

$$(\beta - \alpha)\ (T_o - T_c) \ . \tag{B-4}$$

The unbalance in temperature now existing between the zero mode and the calibrate mode can be expressed as:

$$(\beta - \alpha)\ (T_c - T_E) \ . \tag{B-5}$$

This temperature can be balanced out by injection of noise from a noise generator into the proper antenna transmission line. After balance has been achieved the noise tube can be used to check the gain of the radiometer periodically by switching to zero mode.